Studies of dissolution solutions of ruthenium metal, oxide and mixed compounds in nitric acid

F. Mousset [1], C. Eysseric [1], F. Bedioui [2]

[1] *CEA DEN/SE2A, Valrhô-Marcoule, BP 17171, 30207 Bagnols-sur-Cèze Cedex, France*
[2] *Laboratoire de Pharmacologie Chimique et Génétique, FRE CNRS-ENSCP n°2463, École Nationale Supérieure de Chimie de Paris, 11 rue Pierre et Marie Curie, 75231 Paris Cedex 05, France*

Abstract *– Ruthenium is one of the fission products generated by irradiated nuclear fuel. It is present throughout all the steps of nuclear fuel reprocessing—particularly during extraction—and requires special attention due to its complex chemistry and high* $\beta\gamma$ *activity. An innovative electrovolatilization process is now being developed to take advantage of the volatility of* RuO_4 *in order to eliminate it at the head end of the PUREX process and thus reduce the number of extraction cycles. Although the process operates successfully with synthetic nitrato-*$RuNO^{3+}$ *solutions, difficulties have been encountered in extrapolating it to real-like dissolution solutions. In order to better approximate the chemical forms of ruthenium found in fuel dissolution solutions, kinetic and speciation studies on dissolved species were undertaken with* RuO_2,xH_2O *and Ru° in nitric acid media.*

INTRODUCTION

Ruthenium is one of the chemical elements present in solutions treated in nuclear fuel reprocessing based on the PUREX process. It exhibits specific behavior during the process because of its relative abundance (6% of fission products), high activity (due to isotopes ^{103}Ru and ^{106}Ru) and complex chemistry (more than 25 species at several oxidation states). Multiple oxidation and coordination states of ruthenium are present in the nitric acid media and encountered in reprocessing, including nitrato complexes of nitrosyl ruthenium, colloids with organophosphates in liquid phases, and ruthenium tetroxide (RuO_4) in the off-gas. In an advanced reprocessing concept it would be an improvment to separate the ruthenium from the concentrated flows during the early process steps.

Methods for removing ruthenium within the PUREX process have thus been developed for synthetic or high-level waste solutions. Their principle consists in first oxidizing ruthenium species to the volatile RuO_4 form, followed by selective separation. Oxidation can be performed either by adding a strong oxidant [1] ($KMnO_4$, $K_2Cr_2O_7$ or ozone) or electrochemically [2,3]. The resulting RuO_4 is then removed by precipitation as insoluble RuO_2 through electrochemical reduction or using chemical reducing agents such as hydrazine. This approach involving the use of additional reactants is unsuitable because of the increased quantities of high-level waste requiring subsequent treatment. A simpler and more elegant way is to take advantage of the volatility of RuO_4 to ensure its desorption.

In a context of sustainable development, electrochemistry is well suited for oxidation of the ruthenium species and could be easily coupled with RuO_4 desorption by simple gas flow. An overall conceptual ruthenium separation process has been developed based on two reactions. It consists in oxidizing a synthetic nitrato-nitrosyl-ruthenium complex ($RuNO^{3+}$) in nitric acid, using Ag(II) electrochemically generated at a platinum anode [4-7] as a strong oxidant. The volatile RuO_4 formed is then desorbed from the electrolytic solution by flowing nitrogen and trapped in a suitable liquid phase.

Although the feasibility of a process of this type is well established for the simple synthetic nitrato-nitrosyl-ruthenium $RuNO^{3+}$ solution, further investigation is necessary to better understand the differences observed during extrapolation to nuclear fuel dissolution. For this purpose, RuO_2,xH_2O and Ru° were dissolved in nitric acid for electrovolatilization studies [8]. This paper discusses the speciation and kinetic studies for these simulated dissolution tests.

EXPERIMENTAL

Chemicals

Nitric acid solutions (3N, 6N, 10N) were prepared from concentrated HNO_3 (Merck, *rectapur* grade, 65%). RuO_2,xH_2O powder (x = 4.3, Aldrich; mean particle diameter 11 µm) and Ru° metal powder (Aldrich, micrometric) were used. A solution of nitrato-nitrosyl-ruthenium complex, with the general formula $RuNO(NO_3)_x(NO_2)_y(H_2O)_z^{3-x-y}$ ($x+y+z = 5$), designated $RuNO^{3+}$ in the remainder of this document, was prepared using a commercial powder $RuNO(NO_3)_3$ (Aldrich, 31.3% ruthenium) which is easily dissolved at room temperature in nitric acid. A Ru(IV) standard solution was obtained using H_2O_2 to reduce RuO_4 freshly prepared by dissolution of 5 mM of $KRuO_4$ powder (Aldrich) in concentrated nitric acid. According to Anderson and McConnell [9], the properties of the resulting solution are consistent with the hypothesis that

it contains a series of hydroxo aquo ruthenium complexes of tetravalent ruthenium that could be formulated as $Ru_4(OH)_{12}^{4+}$ and is designated here as Ru(IV). The sodium nitrite solution (7 mol·L^{-1}) is obtained by dissolution of $NaNO_2$ powder (Aldrich) in H_2O (MilliQ).

Analysis of ruthenium solutions

The amount of ruthenium in the dissolution solution was determined by ICP/AES analysis (Jobin Yvon). UV-visible spectrophotometry measurements used to characterize various ruthenium forms as $RuNO^{3+}$ or Ru(IV) were performed with a Cary spectrometer (1A model).

Dissolution Reactor

The dissolutions were carried out in two experimental setups (**Figure 1**). The first series used a four-necked 1L flask and cooler with a Lauda 3°C cryostat. A Bioblock modular heater was used to regulate the dissolution temperature via a temperature sensor immersed in solution. A sampling valve was fitted on one of the necks. The second series of dissolutions was performed with the same setup coupled to a nitrogen oxide (NO_x) generator consisting of a 1 L flask containing 10 N nitric acid heated to 50°C. A 1 mm dia. PTFE connection supplied a 7 mol·L^{-1} sodium nitrite solution from a peristaltic pump to the 10 N nitric acid in the generator to produce nitrogen oxides. They were desorbed by sparging nitrogen at 1.5 L·min^{-1} in the NO_x generator, which was connected via a hermetic line to the dissolution reactor. The vector gas thus carried the nitrogen oxides into the nitric acid dissolution solution, generating nitrous acid *in situ*.

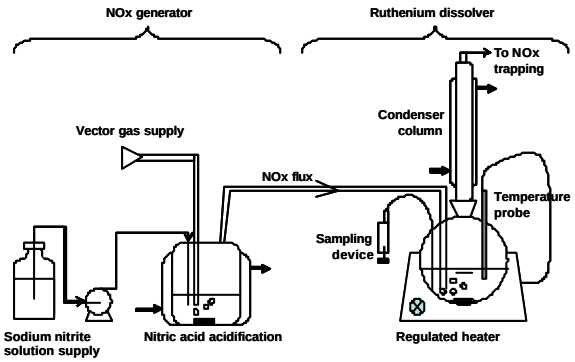

Figure 1. Diagram of the experimental devices

RESULTS AND DISCUSSION

Kinetic studies

The dissolution kinetics was established by ICP-AES determination of the dissolved ruthenium in periodic solution samples. The [Ru] = $f(t)$ curves showed a linear variation during the first 200 minutes, from which an initial dissolution rate r_0 was determined (Figures 1, 2, 3).

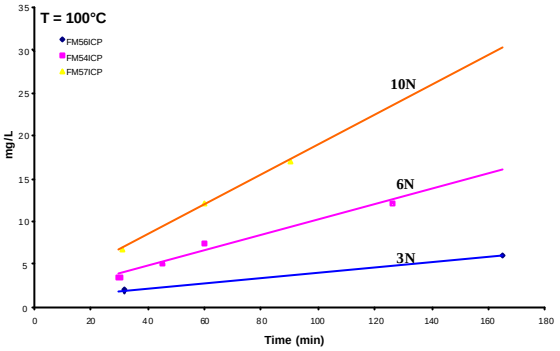

Figure 2. Effect of HNO_3 concentration on the dissolution kinetics of RuO_2,xH_2O at 100°C

Table I. RuO_2,xH_2O dissolution rate (µg·L^{-1}min^{-1}) versus nitric acid concentration and temperature

Temperature	[HNO_3]		
	3 N	6 N	10 N
85°C		3	
100°C	31	90	175
107°C		334	

Figure 2 shows the ruthenium concentration in solution versus time at three acidities (3 N, 6 N and 10 N) during dissolution of RuO_2,xH_2O. The higher the nitric acid concentration, the faster the dissolution kinetics. The dissolution rates are indicated in **Table I**. The results indicated an apparent reaction order of approximately 2 with respect to HNO_3:

$$r_0 \alpha [HNO_3]^2 \quad \textbf{(1)}$$

Figure 3 illustrates the effect of temperature on the dissolution kinetics at 85°C, 100°C and 107°C (boiling) in 6 N HNO_3. The apparent activation energy calculated

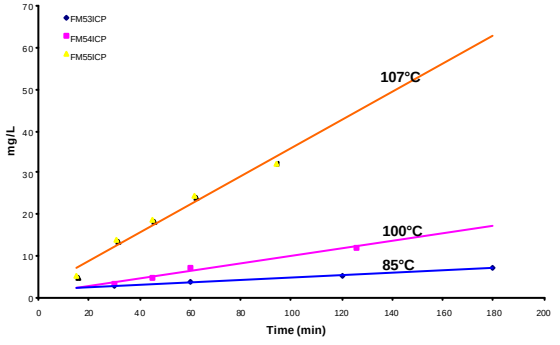

Figure 3. Effect of temperature on the dissolution kinetics of RuO_2,xH_2O, [HNO_3] = 6 N

from these dissolution rates is:

$$E'_a = 246 \text{ kJ/mol} \quad \textbf{(2)}$$

Experiments with NO_x sparging revealed the major influence of this parameter. **Figure 4** shows the variation of the dissolved ruthenium for three different nitrous acid concentrations obtained by increasing NO_x gas generation parameters. The increasing HNO_2 concentration in solution resulted in increased dissolution kinetics as indicated in **Table II**. The apparent order of the nitrous acid concentration was 0.5:

$$r_0 \propto [HNO_2]^{0.5} \quad \textbf{(3)}$$

Table II. RuO_2,xH_2O dissolution rate versus nitrous acid concentration (T = 100°C, $[HNO_3]$ = 6 N)

	$[HNO_2]$ ($\times 10^3$ mol·L^{-1})		
	1.5	4.5	24.5
Dissolution rate (µg·L^{-1}min^{-1})	69	86	268

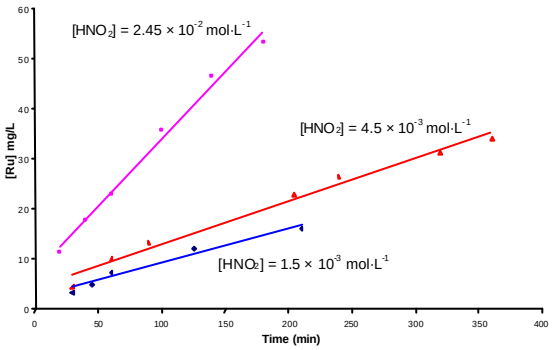

Figure 4. Effect of nitrous acid concentration on the dissolution kinetics of RuO_2,xH_2O, $[HNO_3]$ = 6 N

The relatively low dissolution rates determined under these conditions and the high activation energy are indicative of the difficulty of dissolving the RuO_2,xH_2O powder. By comparison, the dissolution kinetics of the ruthenium contained in spent fuel irradiated are higher than the RuO_2,xH_2O dissolution rates determined during these tests. The significant effect of nitrous acid on the dissolution rates may be one reason for the difference. The standard nitrous acid concentration in a dissolution solution is about 10^{-2} mol·L^{-1}, although a zone of higher concentration may exist at the interface between the fuel and the dissolution solution, where nitrous acid is generated by the dissolution of UO_2. The gas injection method by sparging is unable to reproduce local effects of this type. Co-dissolution studies of UO_2-RuO_2,xH_2O pellets will be planned to investigate this phenomenon.

Moreover, different chemical forms of the initial solid ruthenium can be postulated. It is often assumed [10] that a large fraction of ruthenium in the spent fuel is found as polymetallic compounds alloyed with molybdenum, palladium, rhodium and technetium. These alloys (ε phase) are known as "white inclusions". Initially, dissolution tests were undertaken with micrometer size Ru° metal powder in addition to RuO_2,xH_2O dissolutions. As shown in **Table III**, only high acidity and high temperatures in the presence of nitrous acid are capable of obtaining kinetics that can be quantified by ICP-AES, but remain very slow.

Table III. Dissolution rate r_0 of Ru metal powder for various temperatures, nitric acidities and nitrous acid concentrations

T (°C)	$[HNO_3]$ (N)	$[HNO_2]$ $\times 10^3$ (mol·L^{-1})	r_0 (µg·L^{-1}·min^{-1})
107	3	-	< 0.5
117	10	-	< 0.5
117	10	24.5	4.5

Dissolution tests with polymetallic Ru-Mo and Ru-Mo-Pd alloys are now in progress to identify possible synergistic effects during the dissolution of alloyed elements and to assess the increased representativeness of these alloys compared with spent fuel.

Speciation studies on dissolved species

UV-visible spectrophotometric data obtained from RuO_2,xH_2O dissolution in HNO_3 solutions revealed a mixture of $RuNO^{3+}$ and Ru(IV): $RuNO^{3+}$ absorbs at 471 nm (ε = 50 L·mol^{-1}cm^{-1}) and Ru(IV) at 484 nm (ε = 725 L·mol^{-1}cm^{-1}). The presence of Ru(IV) was corroborated by other electroanalytic studies [8]. A mean molar absorbance coefficient ε_m was determined at an intermediate wavelength (480 nm) by correlating the UV-visible absorbance and the dissolved ruthenium assay by ICP-AES. The relative proportions of $RuNO^{3+}$/Ru(IV) can be determined from (4) and (5) using the Beer-Lambert law.

$$\varepsilon_m = \frac{A}{l \times [\text{Ru}]_{tot}} \quad \textbf{(4)}$$

$$x_{RuNO^{3+}} = \frac{\varepsilon_{Ru(IV)} - \varepsilon_m}{\varepsilon_{Ru(IV)} - \varepsilon_{RuNO^{3+}}} \quad \textbf{(5)}$$

where A is the absorbance at 480 nm, l the optical path length, $[Ru]_{tot}$ the total concentration determined by ICP-AES.

The $RuNO^{3+}$ fraction determined in this way ranged from 36 to 74% for dissolutions without added NO_x.

When the dissolution was performed in the presence of nitrous acid, the $RuNO^{3+}$ fraction exceeded 95%. Nitrous acid thus largely favors the $RuNO^{3+}$ form, and appears to be responsible for the formation of the Ru-NO bond. NO_x was sparged in a commercial Ru(IV) solution to illustrate this hypothesis. Spectrophotometric monitoring confirmed the rapid reduction of Ru(IV) to $RuNO^{3+}$. These observations suggest a simplified two-steps dissolution process for RuO_2,xH_2O in nitric acid:

$$RuO_2,xH_2O + HNO_3 \xrightarrow{HNO_2} Ru(IV)_{sol°} \quad \text{slow} \quad \textbf{(6)}$$

$$Ru(IV)_{sol°} \xrightarrow{HNO_2} RuNO^{3+} \quad \text{fast} \quad \textbf{(7)}$$

CONCLUSION

This study of micrometric RuO_2,xH_2O powder dissolution provided data on the dissolution kinetics of ruthenium in nitric acid alone or with added nitrous acid. It has been shown that nitrous acid is an effective dissolution catalyst: all other conditions being equal, it quadruples the dissolution kinetics. In addition, a spectrophotometric speciation study showed that $RuNO^{3+}$ arises from the action of nitrous acid on Ru(IV), an intermediate dissolution species formed in solution. The rapidity of this reaction confirmed that under the conditions of spent fuel dissolution in the presence of nitrous acid, dissolved ruthenium is stabilized mainly as $RuNO^{3+}$, as previously postulated in the literature.

REFERENCES

1. F.R. Bruce, J.M. Fletcher, H.H. Hyman, editors, *Progress in Nuclear Chemistry,* series III vol. 2, Pergamon Press, pp. 249-250 (1958).
2. K. Motojima, *J. Nucl. Sci. Techn*, **27**, pp. 262 (1990).
3. H.N. Kapur, D.S. Divakar, R.K. Singh, D.D. Bajpai, *Nuclear and Radiochemistry symposium,* December 21-24 India (1992).
4. V. Carron, PhD thesis, Université de Grenoble I – Jospeh Fourier, France (2000).
5. J.M. Adnet, PhD thesis, Institut National Polytechnique de Toulouse, France (1991).
6. D. Espinoux, M. Masson, M. Lecomte, J. Bourges, *Proc. 4th Int. Conf. on Nuclear and Radiochemistry*, September 9-13, Saint-Malo, France (1996).
7. C. Eysseric, D. Espinoux, *Proc. Global'99 Int. Conf.*, Aug 30–Sept 2, Jackson Hole, WY, USA (1999).
8. F. Mousset, F. Bedioui, C. Eysseric, *Electrochem. Comm.*, **6**, pp. 351-356 (2004).
9. J.S. Anderson, J.D.M. McConnell, *J. Inorg. Nucl. Chem.*, **1**, pp. 371 (1955).
10. H. Kleykamp, *J. of Nucl. Mat.*, **131**, pp. 221-246 (1985).